EDMI Microsystems and Microelectronics

MICRO-614: Electrochemical Nano-Bio-Sensing and Bio/CMOS interfaces

Lecture #9

Nanotechnology to enhance Electron Transfer

Lecture Outline

(**Book Bio/CMOS:** Chapter' paragraphs § 8.9.1-4)

- How to integrate CNT
- Electrochemistry of CNT
- Nernst effect with CNT
- Layering effect with CNT
- Cottrell effect with CNT
- Randles-Sevçik effect with CNT
- How to integrate nanoPt (see the Appendix)

CMOS/Sample interface

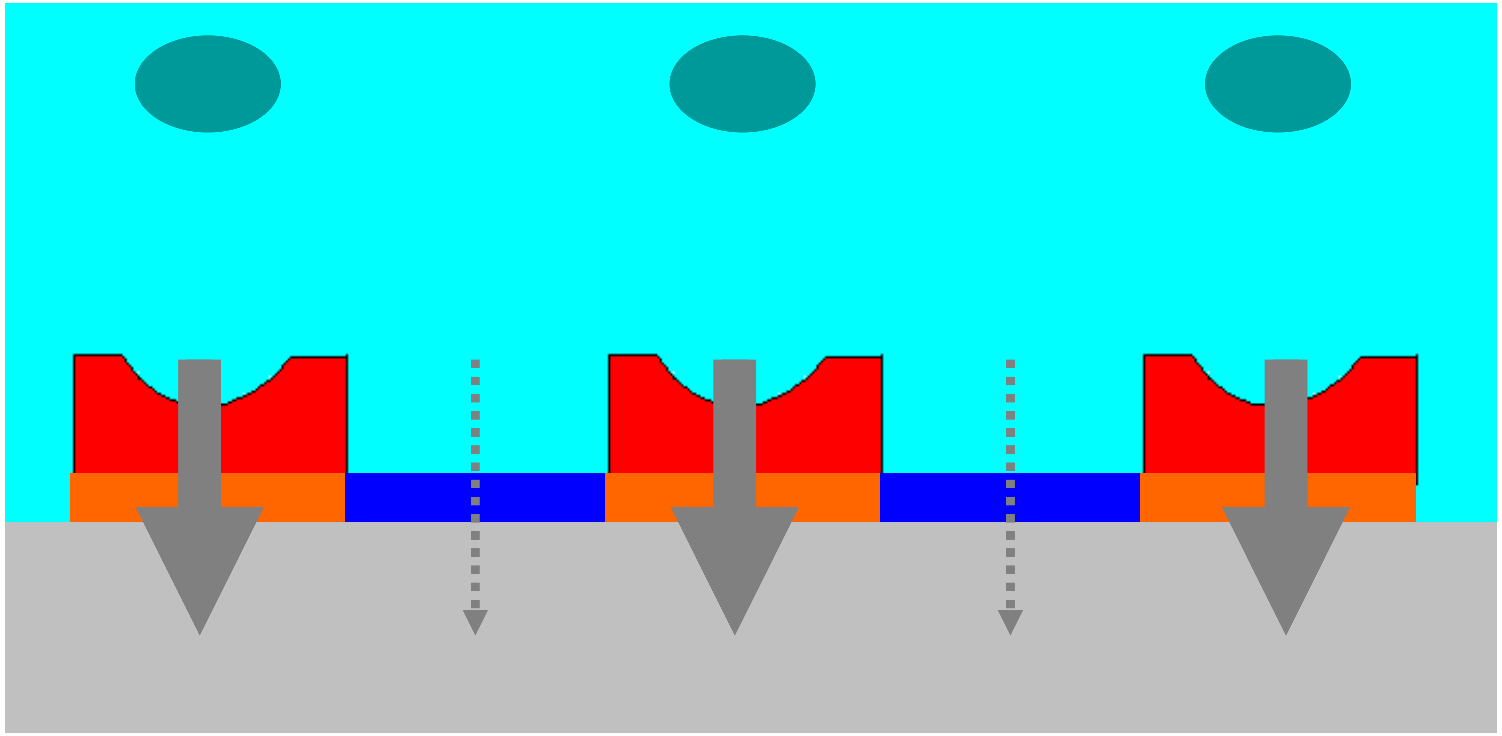

The interface between the CMOS circuit and the bio-sample needs to be deeply investigated and organized

Geometrical Area vs Active Area

$$i(x,t) = \frac{nFA\sqrt{D}C(x,t)}{\sqrt{\pi t}}$$

?

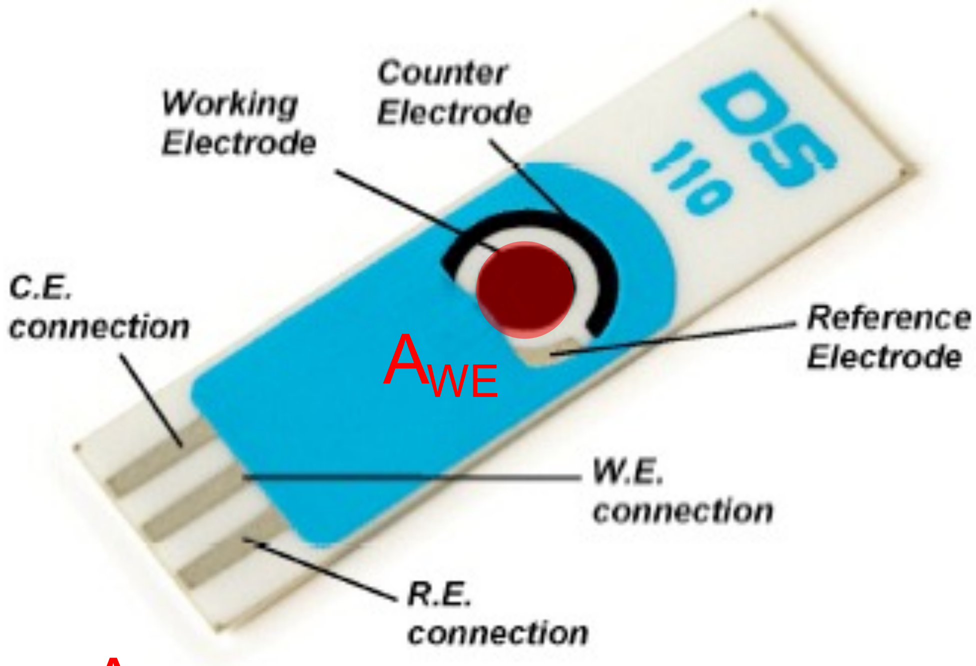

More Active Surface Area

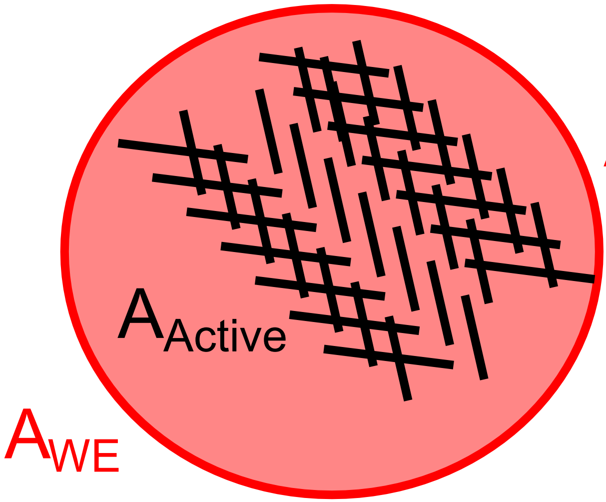

$A_{Active} > A_{WE}$

$$i(x,t) = \frac{nFA_{Active}\sqrt{D}C(x,t)}{\sqrt{\pi t}}$$

Electrochemically Active Area

Carbon Nanotubes (CNT)

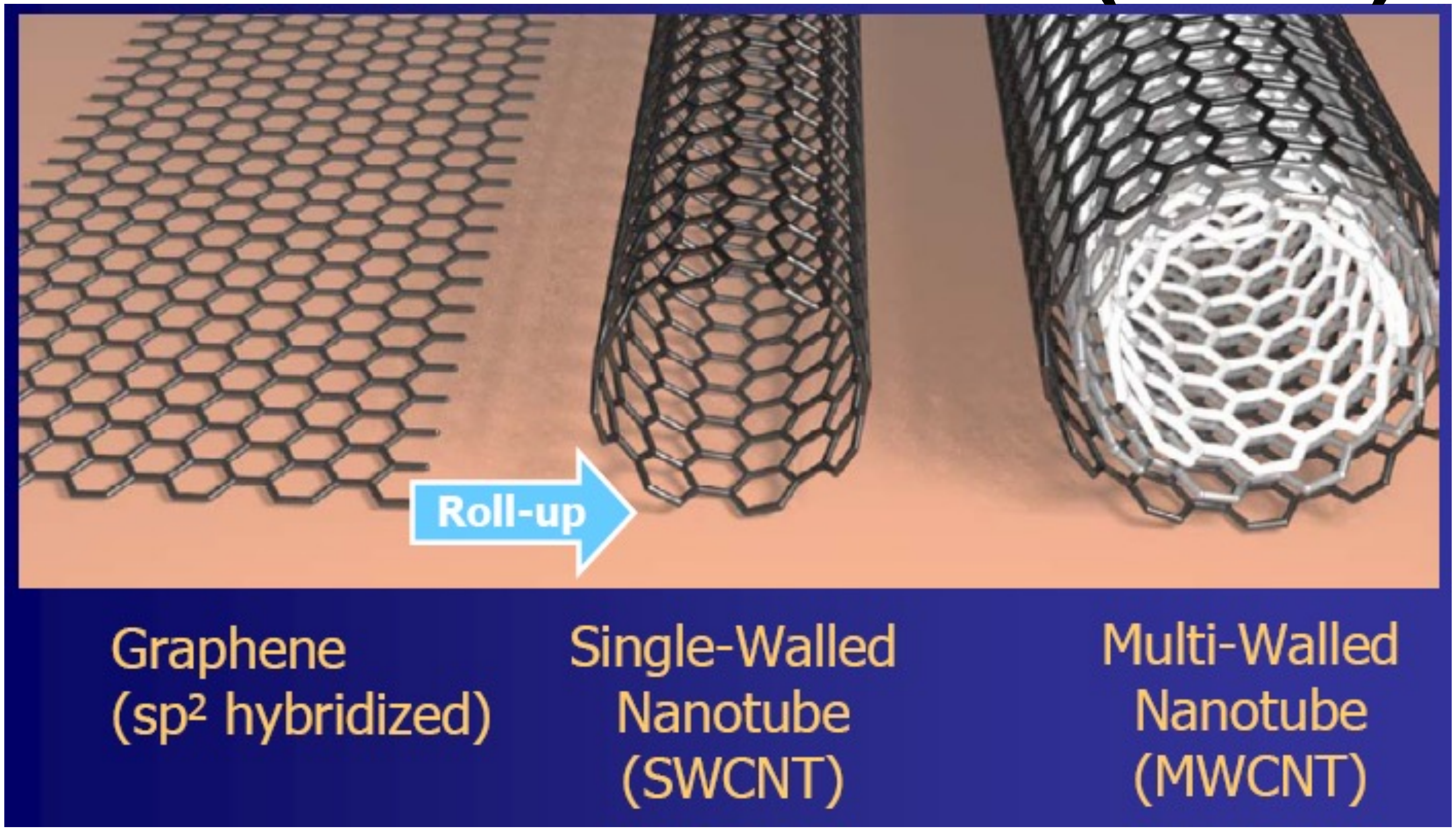

Courtesy: K. Banerjee/California Univ.

CNT electrical conductivity

	Cu	SWCNT	MWCNT
Max current density (A/cm^2)	<1x10^7	>1x10^9 Radosavljevic, et al., *Phys. Rev. B*, 2001	
Thermal conductivity (W/mK)	385	5800 Hone, et al., *Phys. Rev. B*, 1999	3000 Kim, et al., *Phys. Rev. Let.*, 2001
Mean free path (nm) @ room temp	40	>1,000 McEuen, et al., *Trans. Nano.*, 2002	25,000 Li, et al., *Phys. Rev. Let.*, 2005

Single Walled or Multi-Walled Carbon Nanotubes leads to different electrical properties

CNT to improve Bio/CMOS interfaces

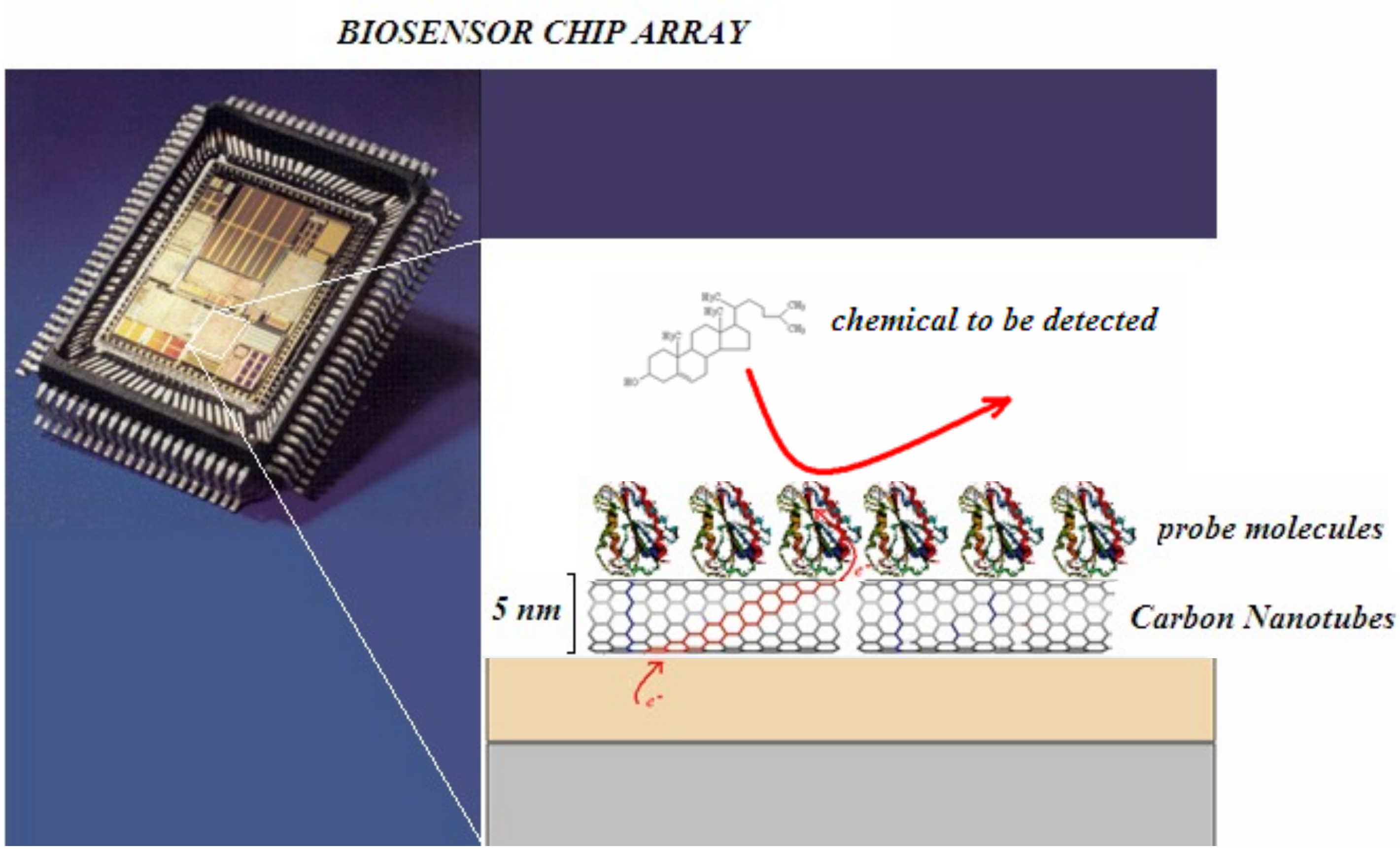

Improvements by Nanotechnology in Label-Free Diagnostics enhance Sensitivity and specificity

Methods for CNT deposition

- Drop casting
- Micro-spotting
- Electrodeposition
- Growth by Chemical Vapour Deposition

CNT integration by Drop-Casting

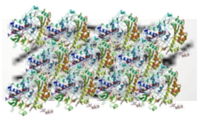

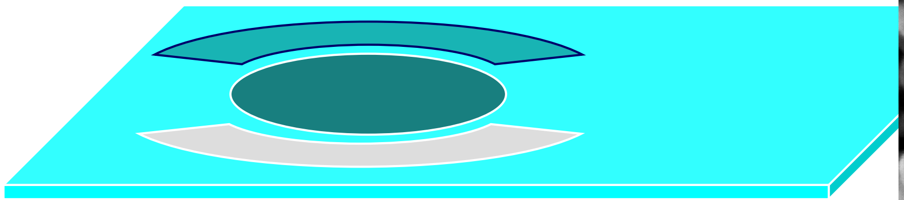

Boero, Carrara et al. / IEEE PRIME 2009
Boero, Carrara et al. / IEEE ICME 2010
De Venuto, al. et Carrara / IEEE Senors 2010
Boero, Carrara et al. / Sensors & Actuators B 2011
Carrara et al. / Biosensors and Bioelectronics 2011
Boero, Carrara et al. / IEEE T on NanoBioScience 2011

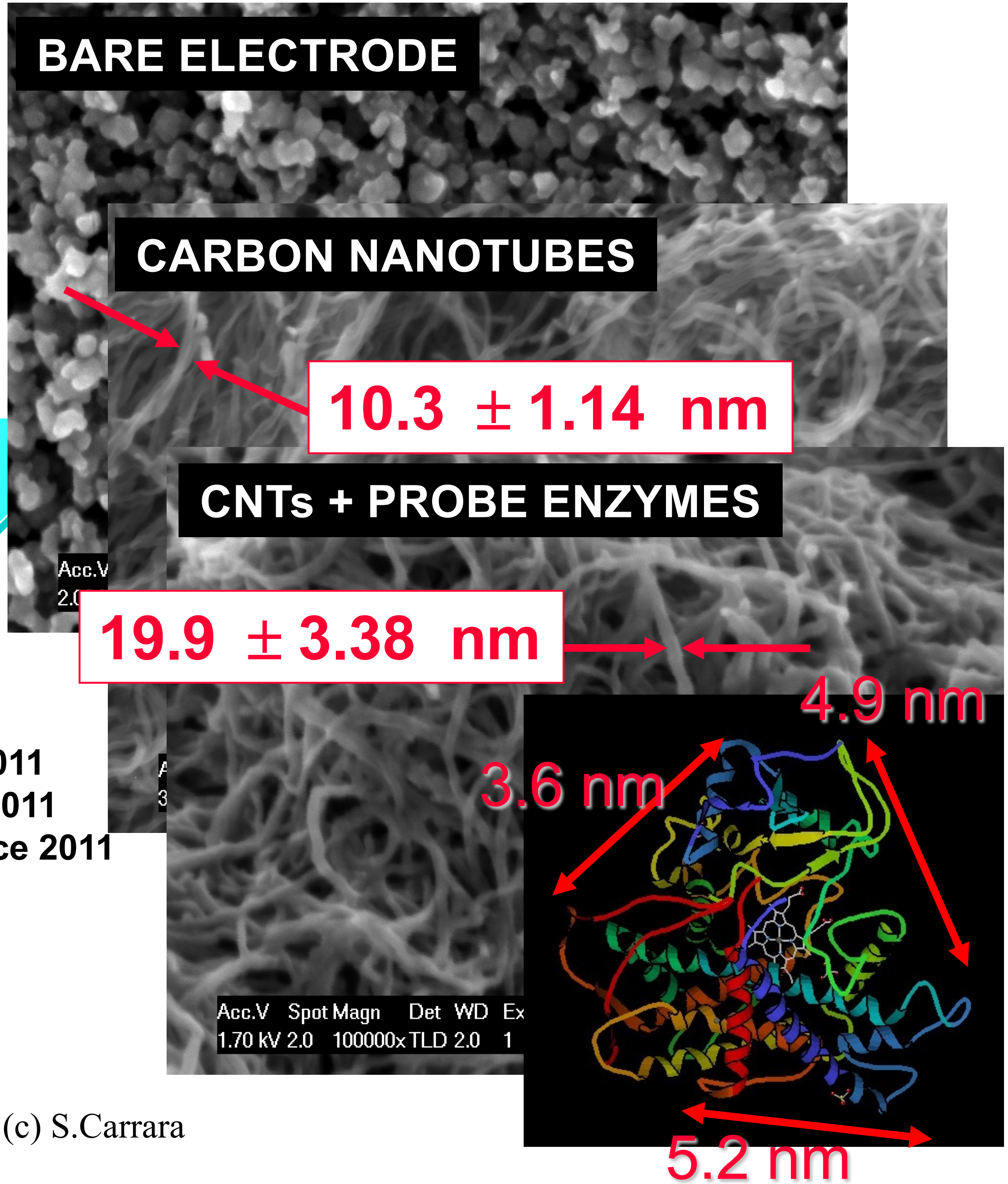

CNT integration by Micro-Spotting

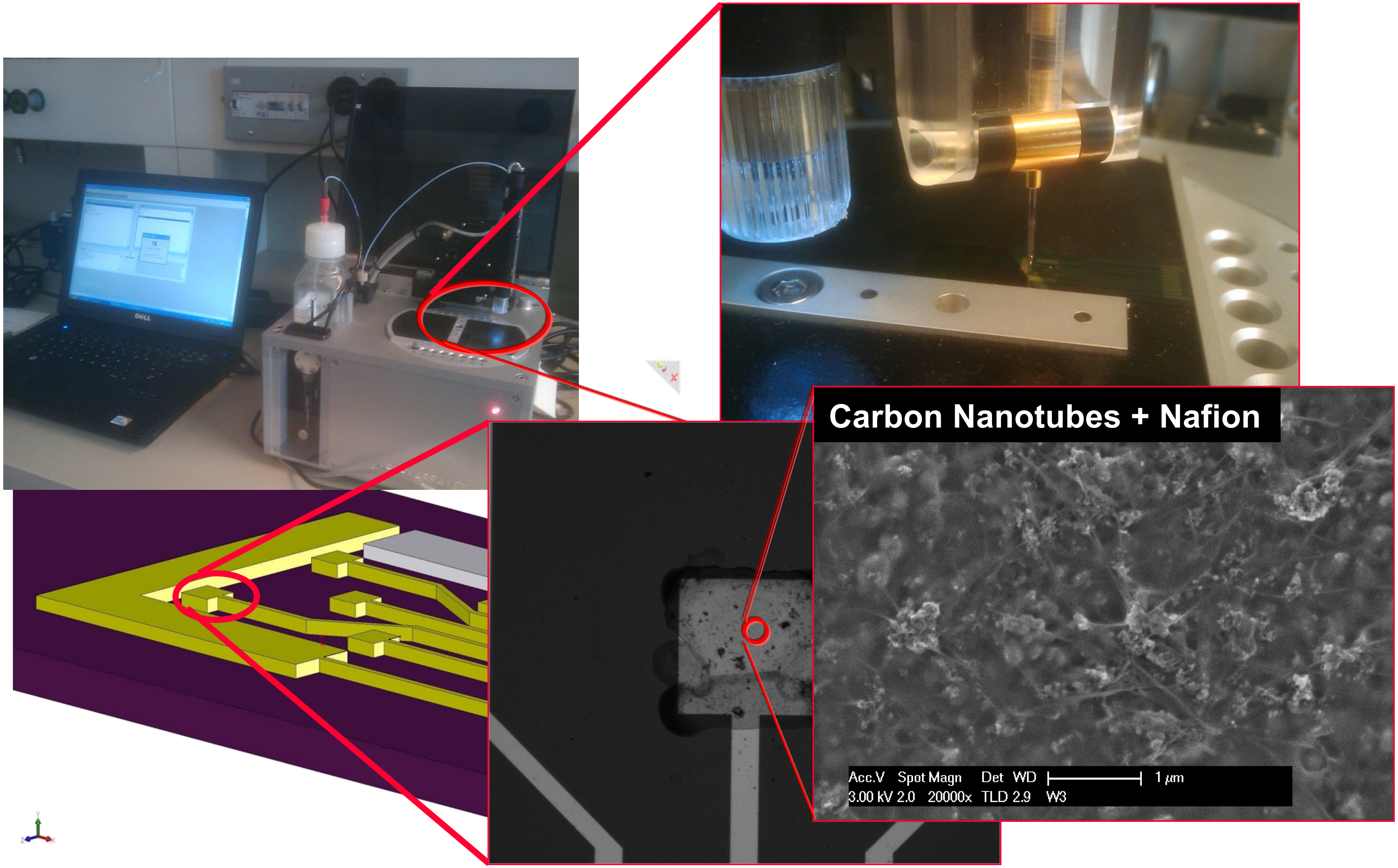

CNT integration by Electrodeposition

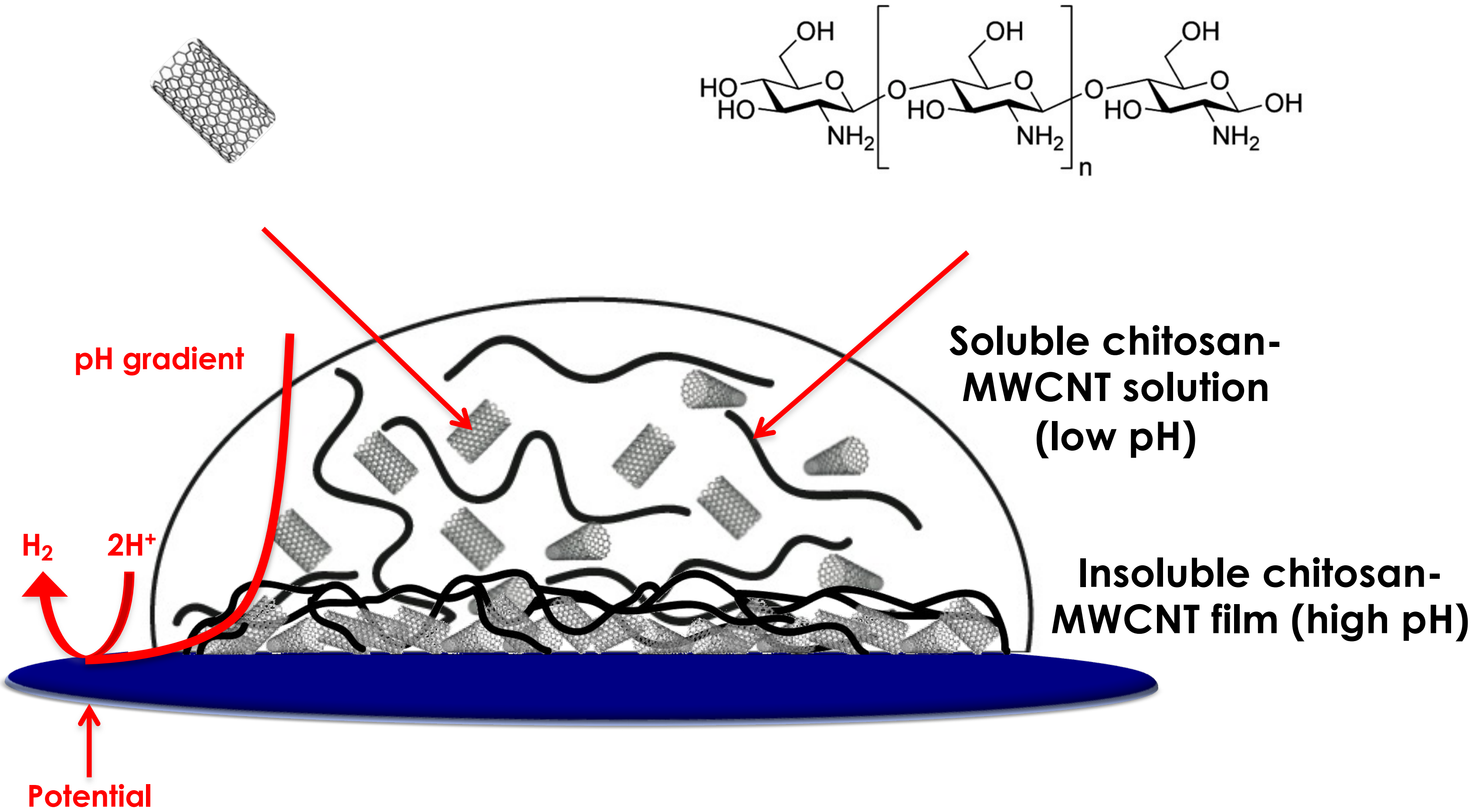

CNT integration by Electrodeposition

DROP-CASTING

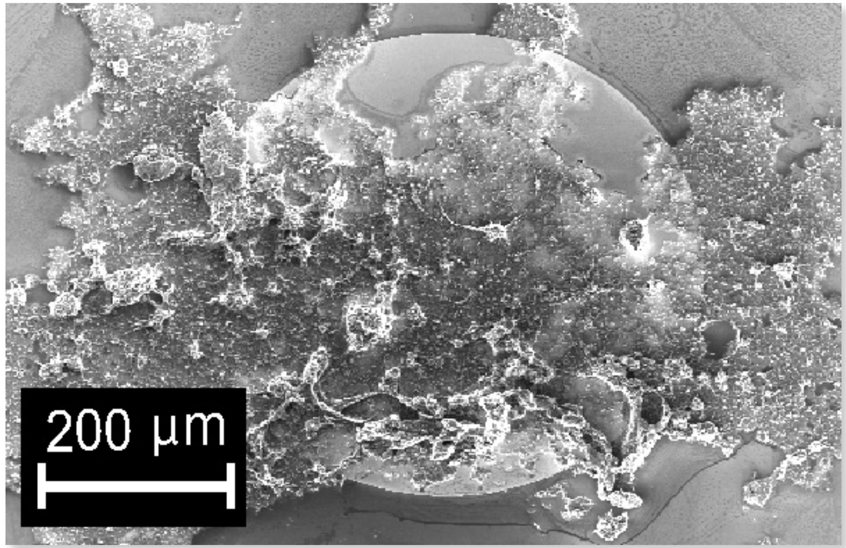

Results

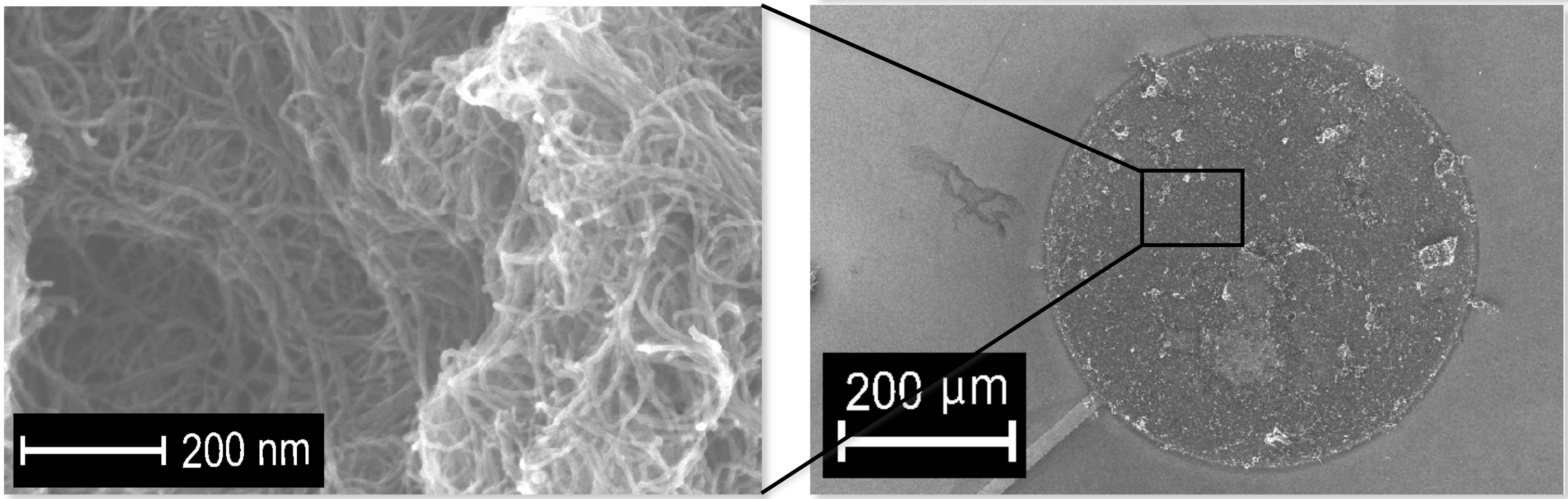

ELECTRODEPOSITION

CNT integration by CVD

Integration by Direct Growth

Step I Catalyst electrodeposition

Step II Annealing (3-10 minutes)

Step III Deposition (CO_2 and C_2H_2 flow)

Taurino, Carrara et al. / UE Patent 2013

Down now till 450 ° C
To be fully CMOS-compatible

Deposition chamber
(750-600 ° C)

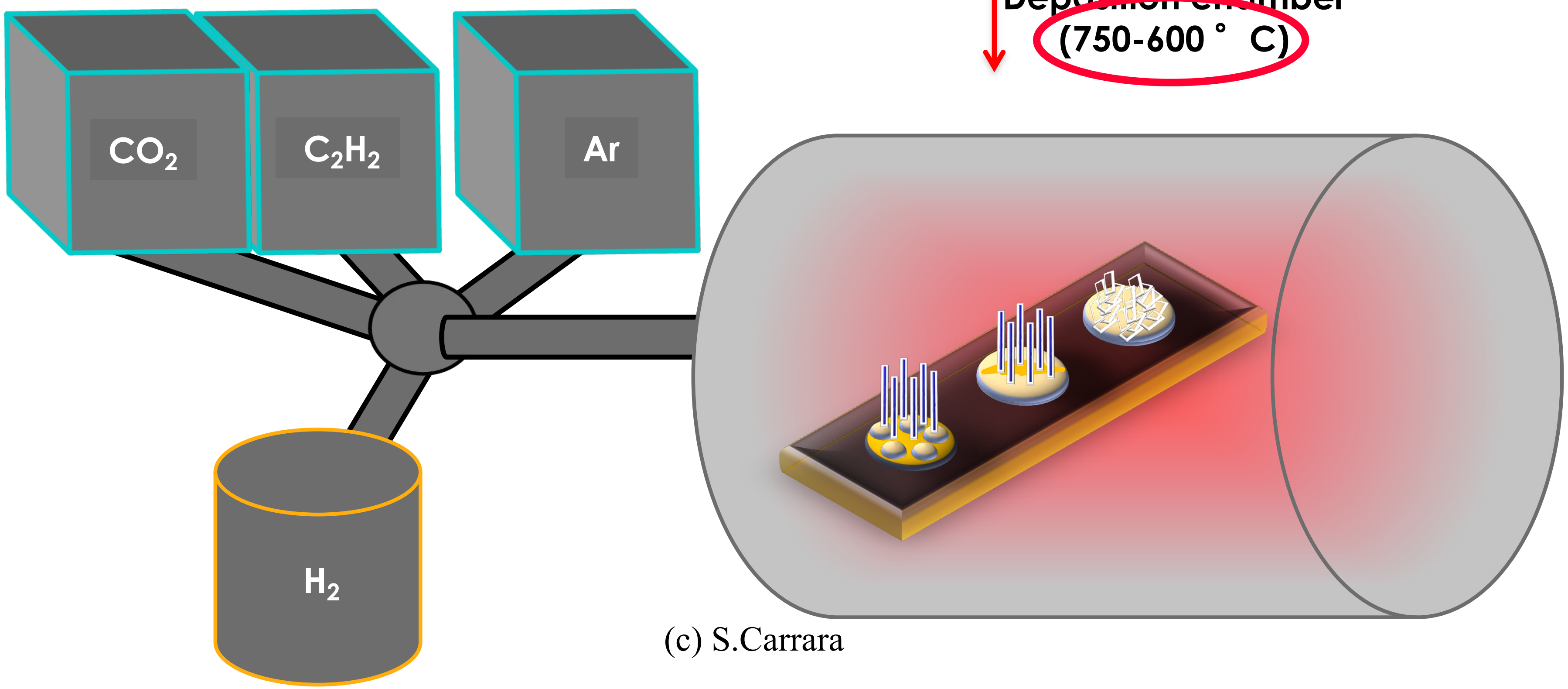

(c) S.Carrara

CNT integration by CVD

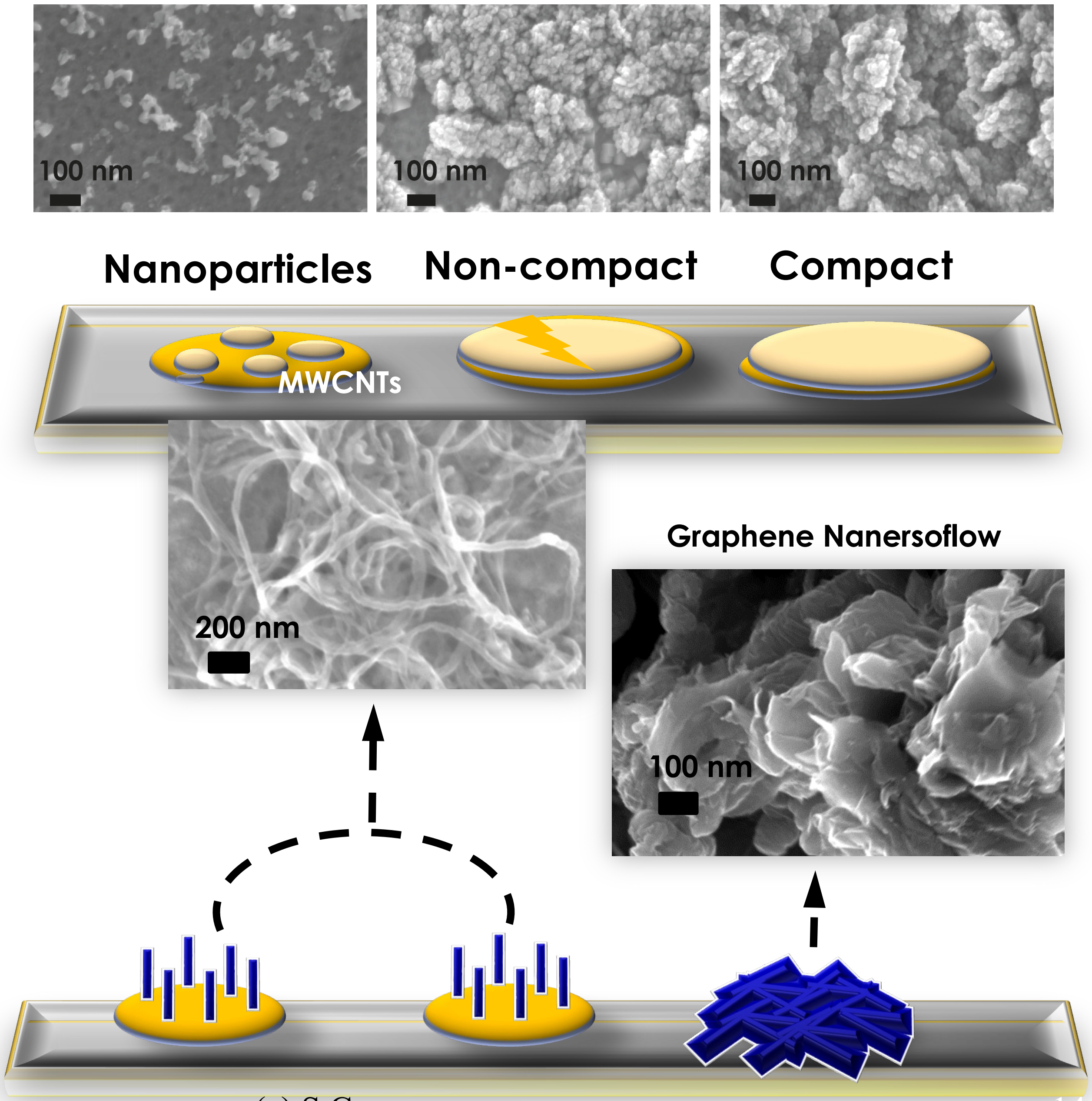

Results

1. Fe electrodeposition

2. Deposition

- *10 min annealing*
- *5 min deposition*
- *750 ° C*
- *0.25 l/h C_2H_2 flow*
- *0.25 l/h CO_2 flow*

CNT integration contribution to Redox Reactions Efficiency

Nernst equation

$$E = E^0 - \frac{RT}{nF}\ln\left(\frac{C_R(0,t)}{C_O(0,t)}\right)$$

Randles-Sevčik equation

$$i(0,t) \propto nFAD\left(\frac{nF\nu D}{RT}\right)^{1/2} C(0,t)$$

Cottrell equation

$$i(x,t) = \frac{nFAD^{1/2}C(x,t)}{\pi^{1/2}t^{1/2}}$$

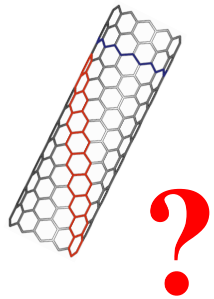

Redox with oxidases

The hydrogen peroxide provide two possible redox reactions. An oxidation:

$$H_2O_2 \xrightarrow{+650mV} 2H^+ + O_2 + 2e^-$$

And a reduction:

$$H_2O_2 + 2H^+ + 2e^- \xrightarrow{+1540mV} 2H_2O.$$

A third redox is provided by the oxygen reduction:

$$2O^+ + 2e^- \xrightarrow{-700mV} O_2.$$

Redox with hydrogen peroxide

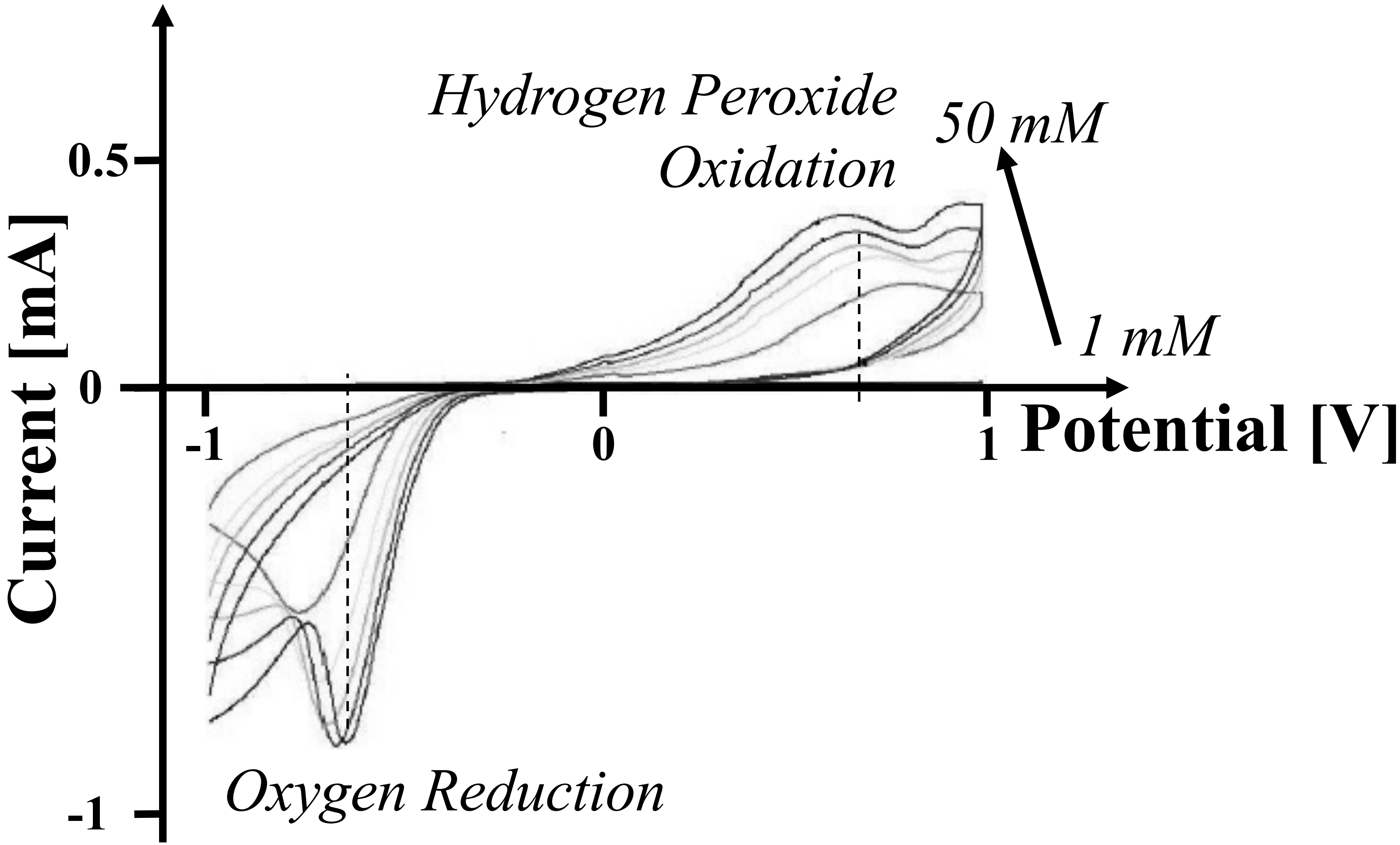

Nernst Effect on H_2O_2 oxidation

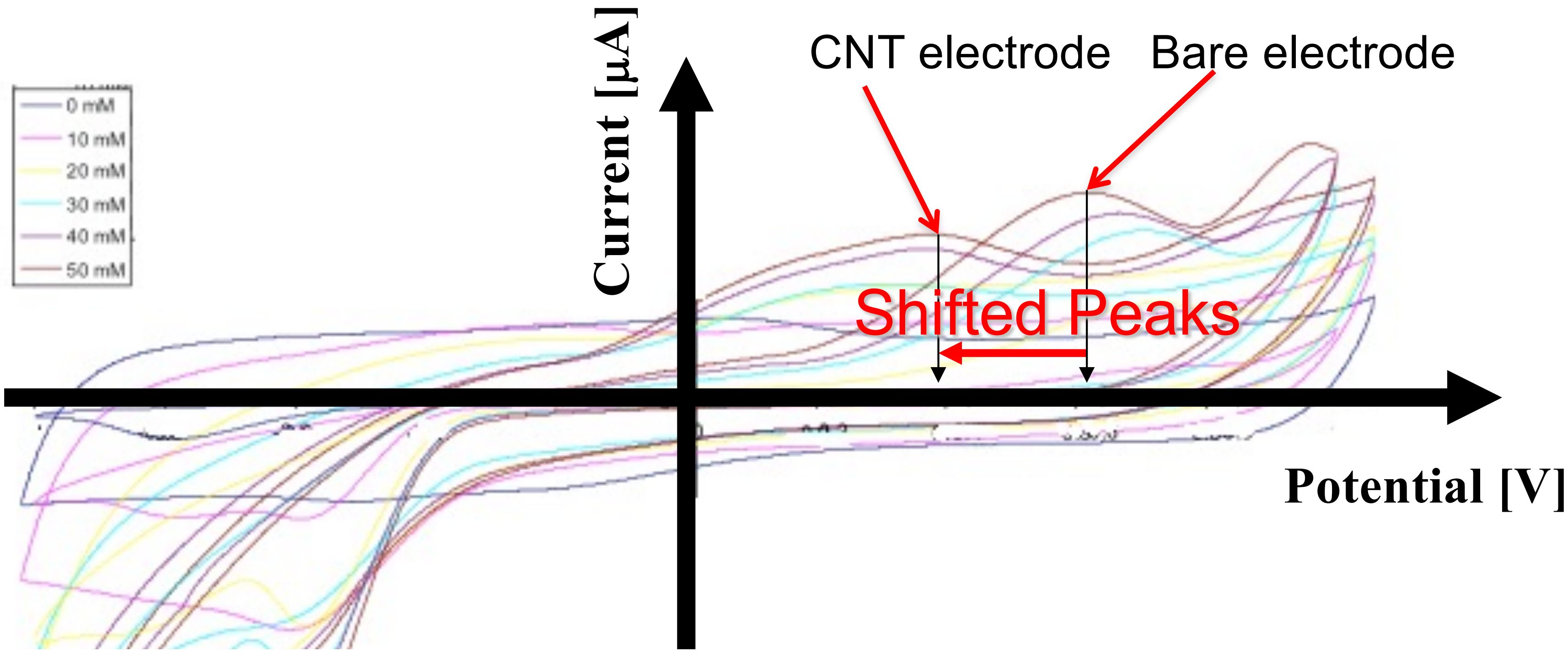

Table 3
Largely evident Nernst effect on H_2O_2.

H_2O_2 Concentration	Bare		CNT	
	Current (µA)	*Potential (mV)*	*Current (µA)*	*Potential (mV)*
10 mM	3.9 ± 0 1	706±0.4	9.1+1.6	174 ± 2.7
20 mM	23.7 ± 0.1	682±0.3	37.0 ± 1.9	204 ± 0.8
30 mM	49.5 ± 0.2	665±0.3	70.5 ± 1.3	230 ± 0.8
40 mM	55.0 ± 0.2	623±0.4	103.5 ± 2.4	291 ± 0.5
50 mM	64.4 ± 0.3	572±0.3	115.0 ± 2.7	284 ± 0.5

S. Carrara et al. / Electrochimica Acta 128 (2014) 102–112

Nernst Effect on O_2 reduction

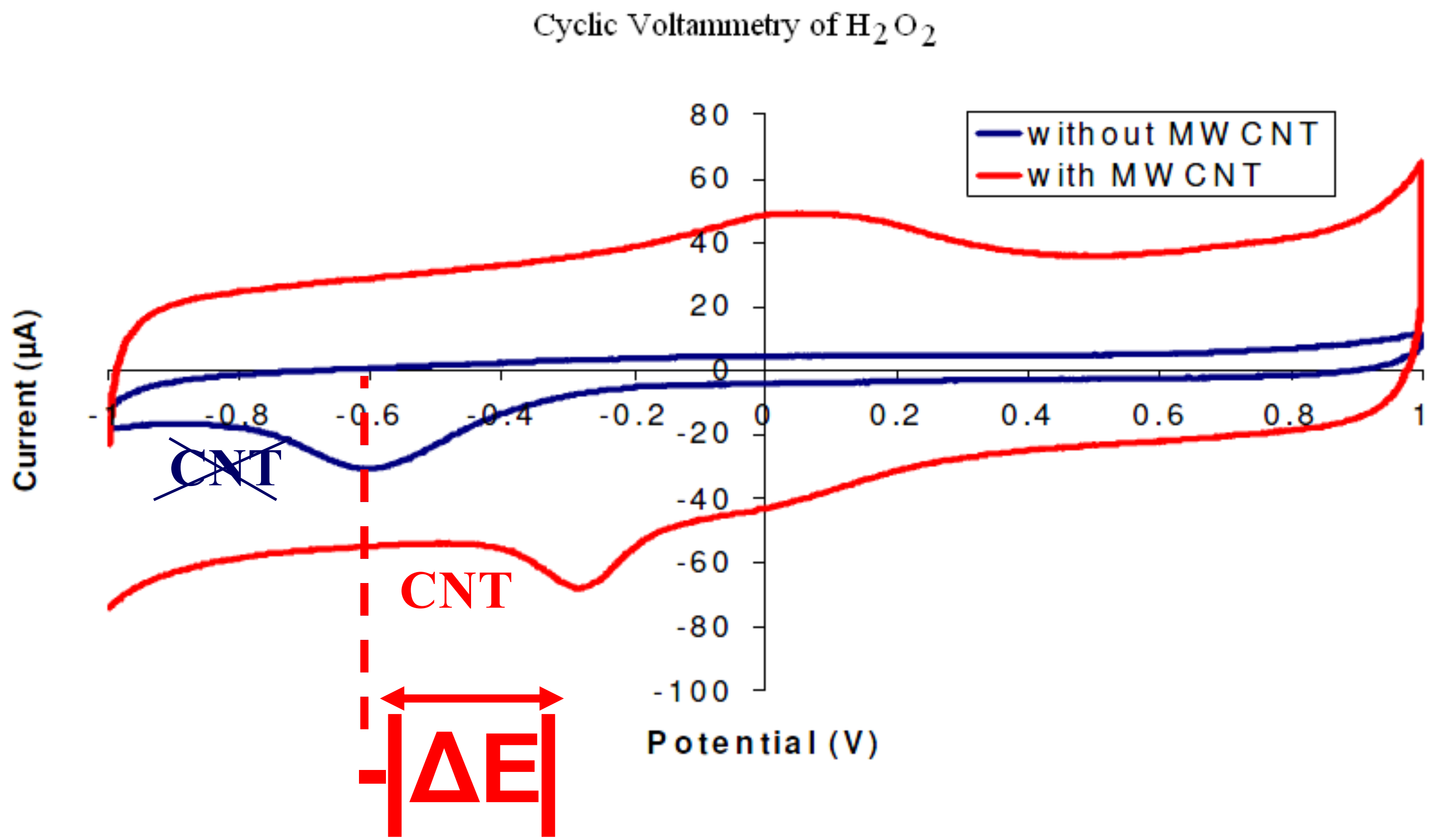

The peak potential is shifted toward lower potentials in case of electrons-transfer is mediated by carbon nanotubes

Nernst Effect on P450 2B4

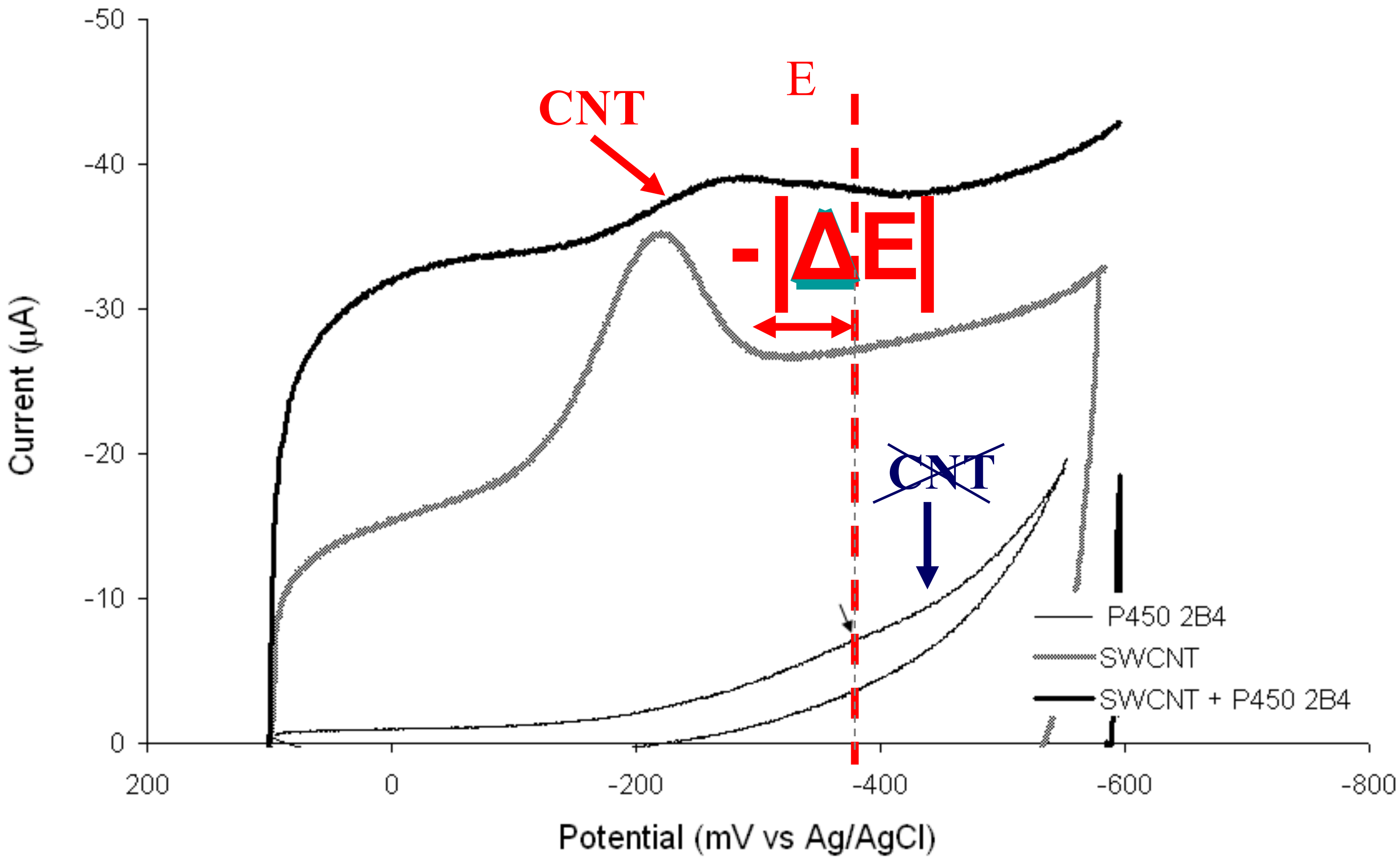

The peak potential is shifted toward lower potentials in case of electrons-transfer is mediated by carbon nanotubes

Nernst effect on different P450s

Table 1
Randle-Sevcick effect and clear Nernst effect on Cyclophosphamide by P450 2B6.

Cyclophosphamide Concentration	Bare		CNT	
	Current (µA)	*Potential (mV)*	*Current (µA)*	*Potential (mV)*
1 mM	0.51 ± 0.01	-302.1 ± 1.9	0.64 ± 0.01	-285.0 ± 3.8
2 mM	0.50 ± 0.01	-299.7 ± 1.9	0.77 ± 0.00	-280.1 ± 1.1
3 mM	0.52 ± 0.01	-294.8 ± 1.7	1.03 ± 0.01	-265.5 ± 3.6
4 mM	0.53 ± 0.01	-299.7 ± 2.0	1.51 ± 0.01	-265.5 ± 3.8
5 mM	0.51 ± 0.01	-298.5 ± 2.6	1.99+0.01	-248.4 ± 3.6

Table 2
Randle-Sevčick effect and clear Nernst effect on Cyclophosphamide by P450 3A4.

Cyclophosphamide Concentration	Bare		CNT	
	Current (µA)	*Potential (mV)*	*Current (µA)*	*Potential (mV)*
1 mM	0.82±0.01	-288.6±3.8	1.54±0.01	-221.1 ± 7.7
2 mM	0.82±0.01	-279.7±2.8	1.59±0.02	-220.5 ± 8.7
3 mM	0.84±0.01	-272.7±3.1	1.60±0.01	-222.1 ± 7.3
4 mM	0.86±0.01	-264.4±2.9	2.12±0.01	-225.7 ± 4.6
5 mM	0.85±0.01	-262 2±3 1	3 02±0.01	-223.6 ± 4.6

S. Carrara et al. / Electrochimica Acta 128 (2014) 102–112

Peak position by Ernst

the position (E) of the redox and oxidation peaks of a species is related to the standard potential (E0) and to the concentration of the species in oxidized and reduced forms by the well-known Nernst equation

$$E_{Nerst} = E_0 + \frac{RT}{nF} \ln \left[\frac{C_o}{C_R} \right]$$

Peak position by Thin-layer effect

However, the semi-infinite planar diffusion model does not work when dealing with nano-structuring. In this case, the phenomenon is more accurately explained by thin-layer effects, which foresees a fully irreversible electron transfer system as driven by

$$E = E_{Nerst} + \frac{ET}{\alpha F} \ln\left(\frac{\alpha F \upsilon}{RTlk_0}\right)$$

l is the thickness of the thin layer,α and k0 are the usual transfer coefficient and standard heterogeneous rate constant, respectively

CNTs contribution to Surface Concentration and Layering Effects

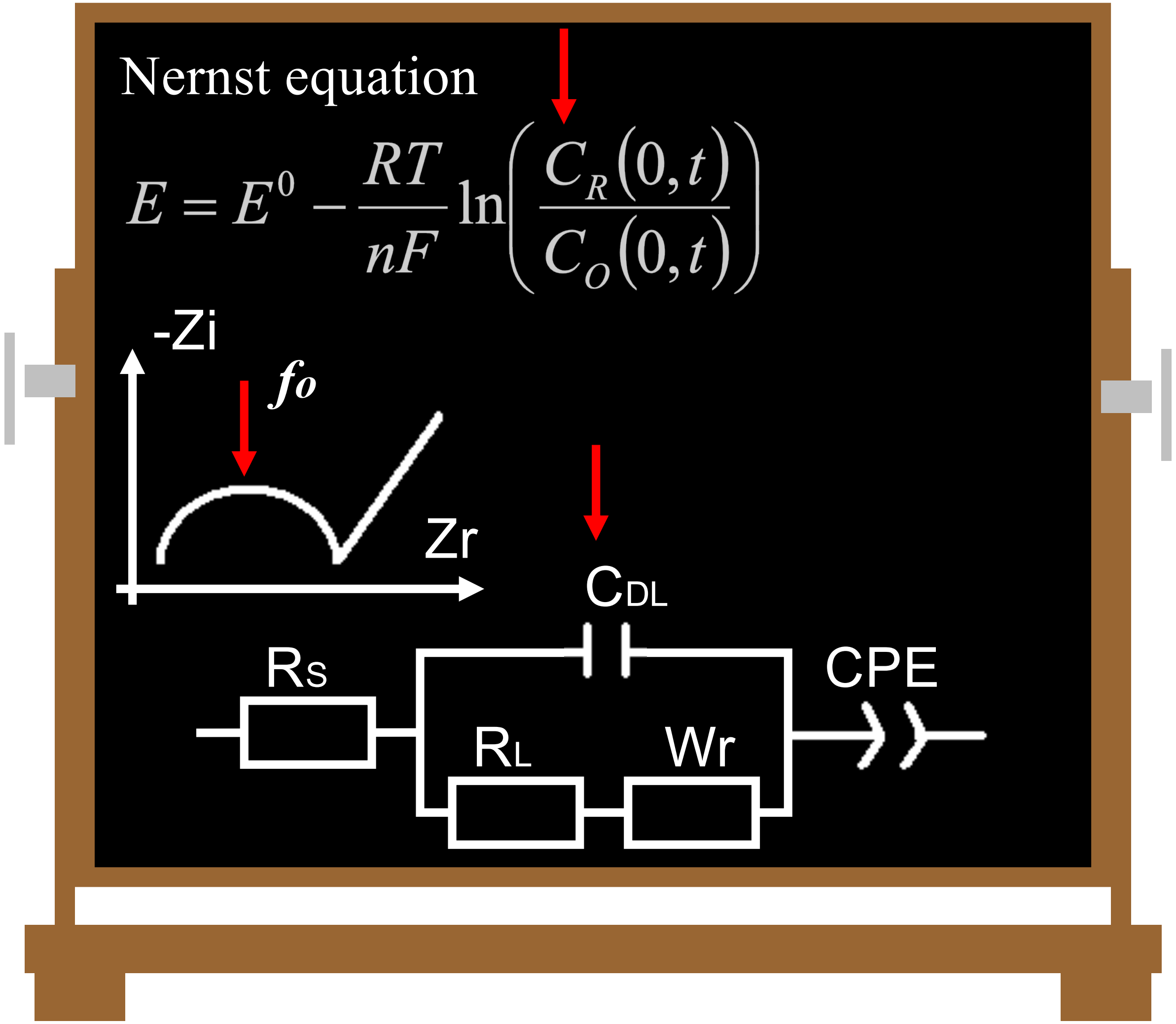

AFM on CNT & polymers

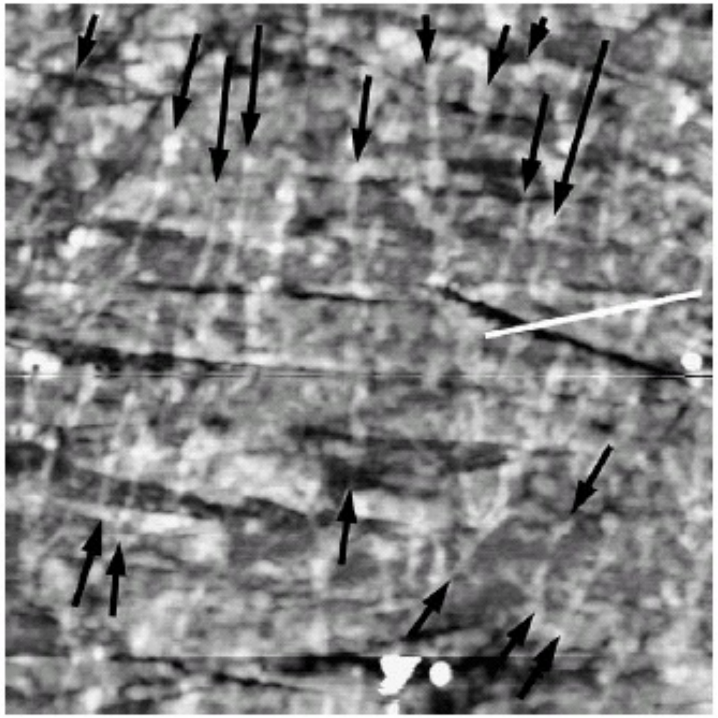

S. Carrara et al. / Sensors and Actuators B 109 (2005) 221–226

Poly-(ortho)-anisidine (POAS)

polyaniline derivatives have not the tendency to form well organized films, as it was shown by AFM microscopy
(Ram M.K., et al., Synthetic Metals 100(1999) 249-259)

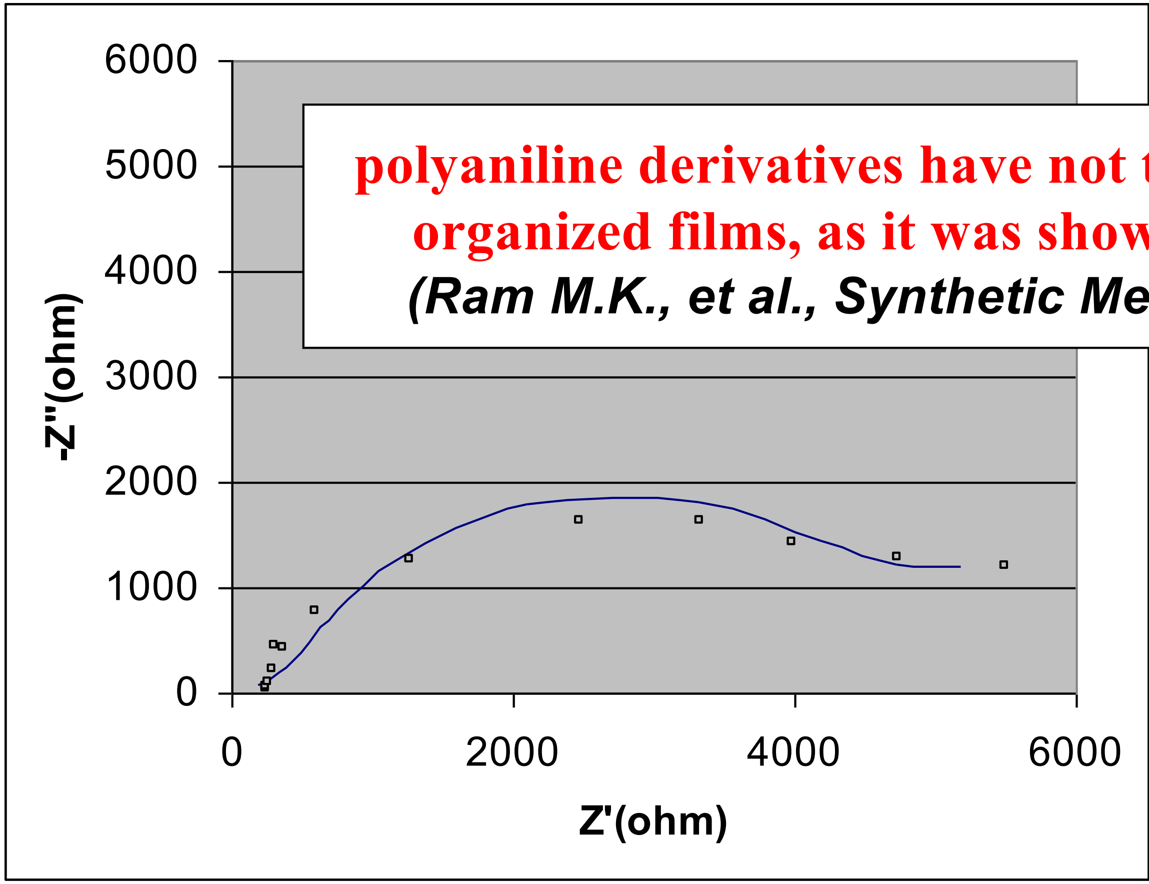

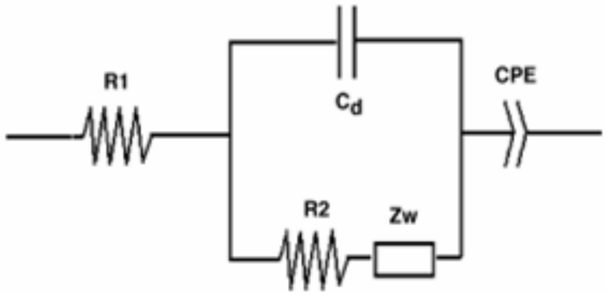

Nyquist impedance diagram of a pure POAS film

Conducting Polymer + Carbon Particles

Consistent with the Lundberg Theory of conducting mixtures

(B.Lundberg, B.Sundqvist, J.Appl.Phys. 60(1986) 1074-1079)

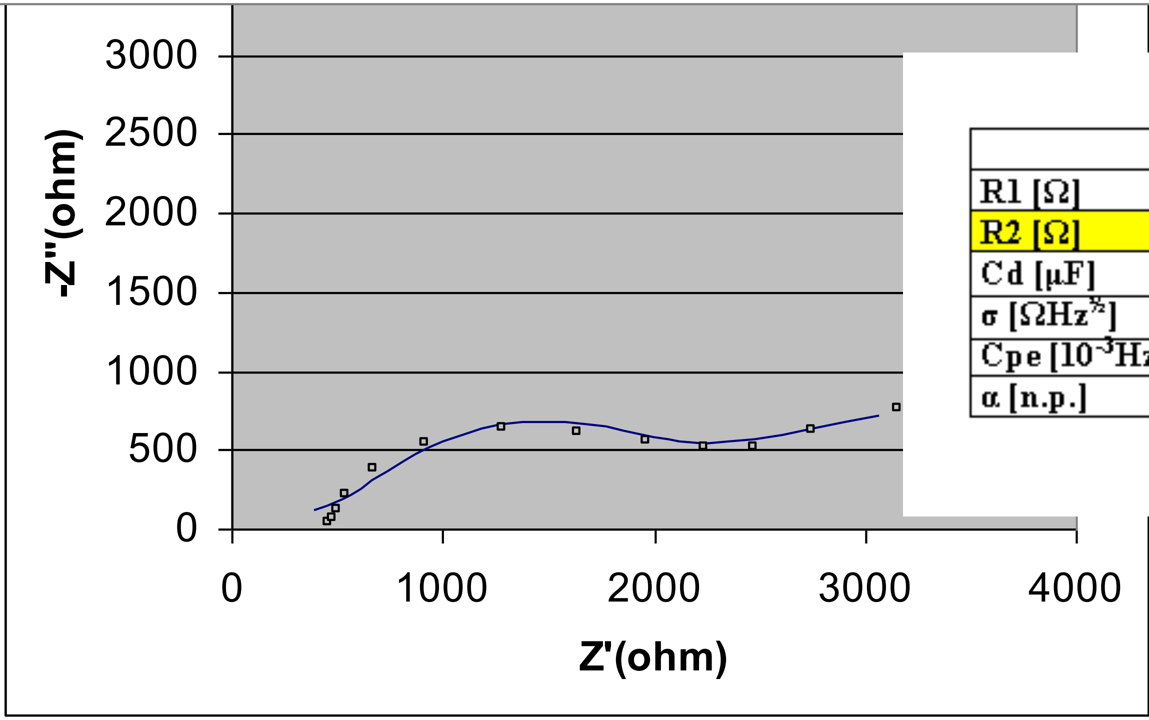

	POAS	POAS+CB
R1 [Ω]	46	64
R2 [Ω]	3165	869
Cd [μF]	32.7	23.3
σ [$\Omega Hz^{½}$]	353	252
Cpe [$10^{-3} Hz^{\alpha}/\Omega$]	0.57	0.49
α [n.p.]	0.298	0.207

decrease of the charge transfer resistance

Nyquist impedance diagram of a POAS film. Experimental data are showed by boxes. Data are acquired in the frequency range from 1KHz down to 100mHz. The solid line shows the best fitting

Conducting Polymer + Multi Walled CNTs

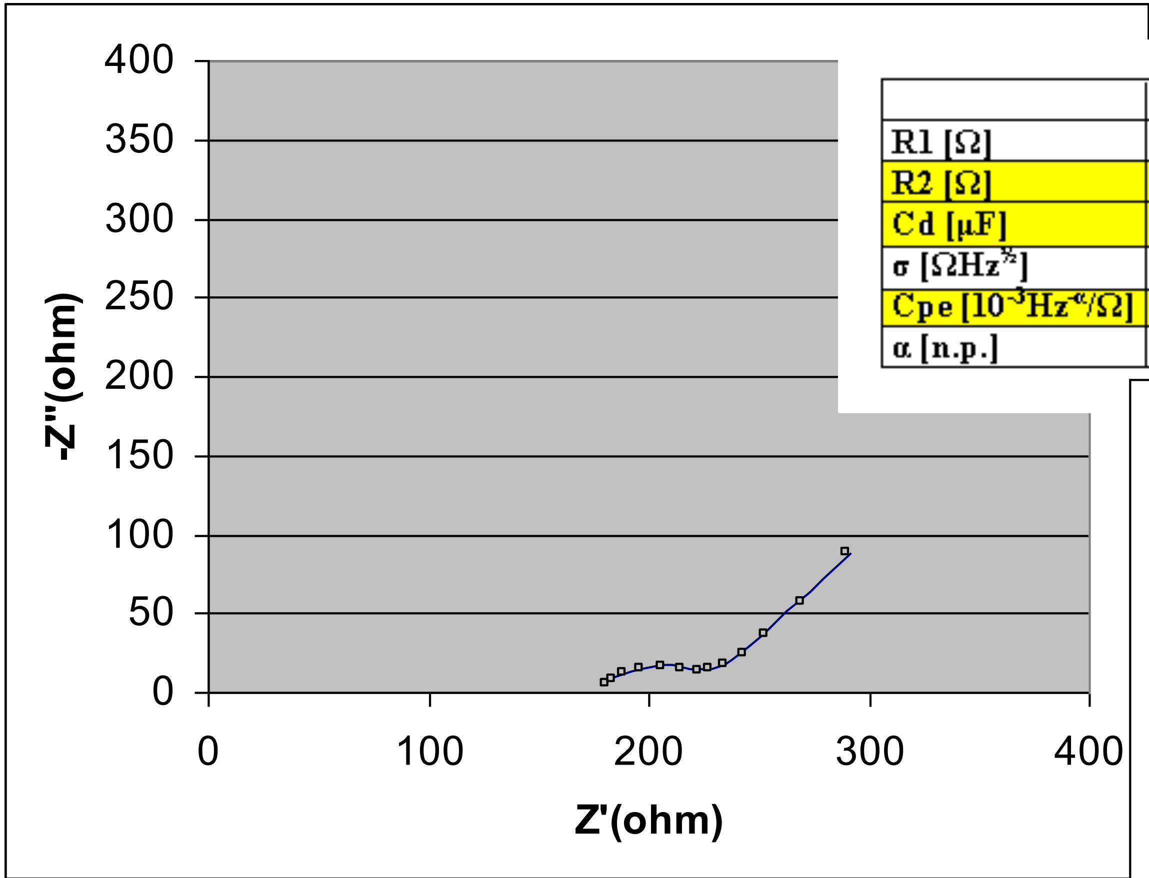

S.Carrara et al., Sensors and Actuators B: Chemicals 109 (2005) 221-226

	POAS	POAS+NT
R1 [Ω]	46	173
R2 [Ω]	3165	50
Cd [μF]	32.7	117.1
σ [$\Omega Hz^{1/2}$]	353	215
Cpe [$10^{-3} Hz^{\alpha}/\Omega$]	0.57	11.68
α [n.p.]	0.298	.575

Pure electrostatic attraction in the double layer and faradic reaction are responsible for the super-capacitance phenomena in Carbon Nanotubes structures

Pan et al., Chem. Mater., Vol. 19, No. 25, 2007

- Nyquist impedance diagrams of a POAS film synthesized with Carbon Nanotubes. Experimental data are showed by boxes. Data are acquired in the frequency range from 1KHz down to 100 mHz. The solid line shows the best fitting

Carbon Nanotubes contribute to Redox Reactions Efficiency

Nernst equation

$$E = E^0 - \frac{RT}{nF}\ln\left(\frac{C_R(0,t)}{C_O(0,t)}\right)$$

Randles-Sevčik equation

$$i(0,t) \propto nFAD\left(\frac{nF\nu D}{RT}\right)^{1/2} C(0,t)$$

Cottrell equation

$$i(x,t) = \frac{nFAD^{1/2}C(x,t)}{\pi^{1/2}t^{1/2}}$$

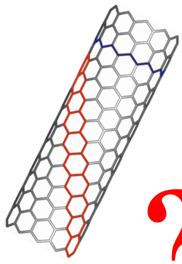

?

Cottrell Effects on H_2O_2

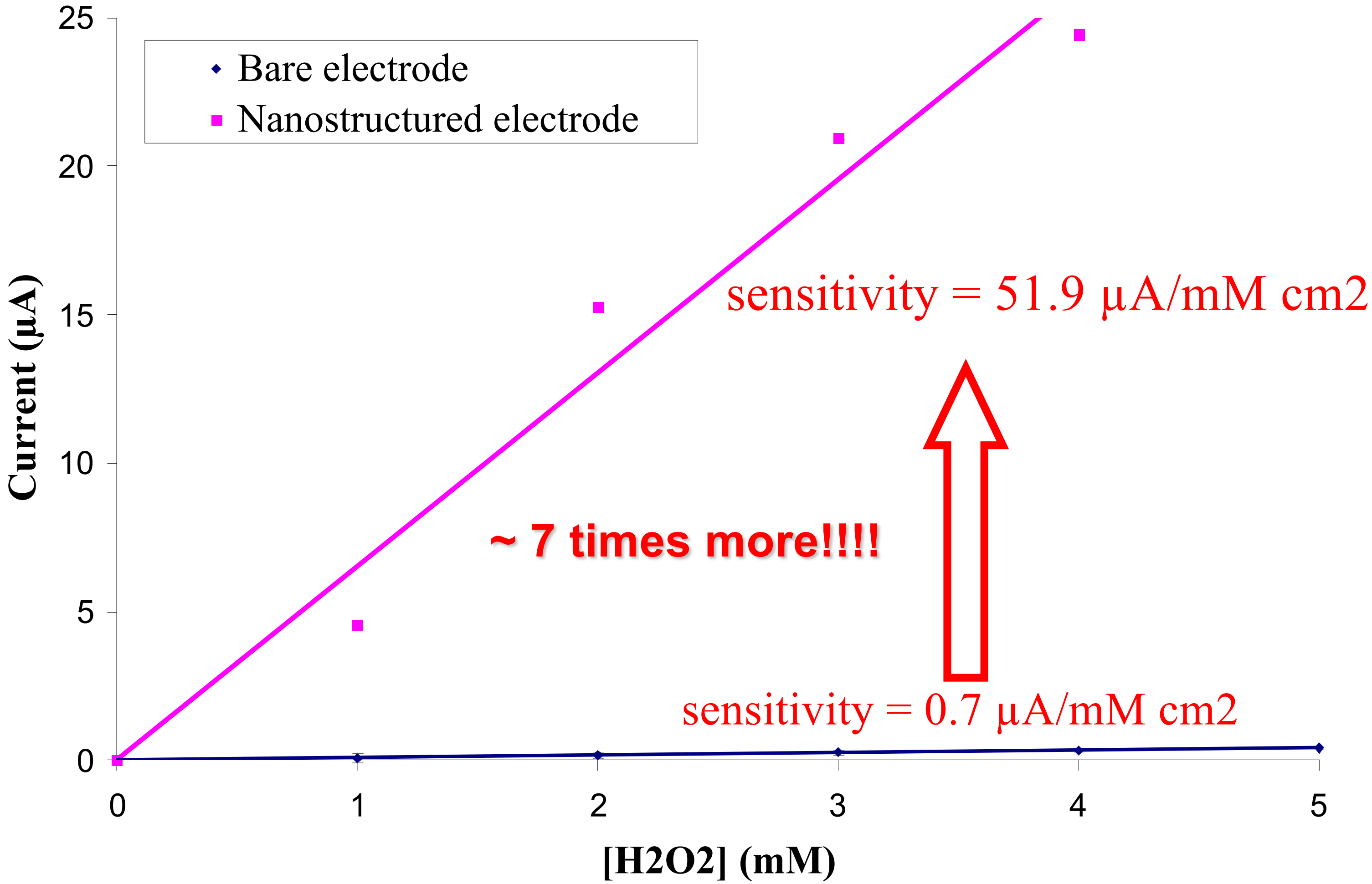

Peroxide Detection

TABLE I

SENSITIVITY VALUES FROM LITERATURE

Methods	Sensitivity
Au-Nafion®- TNTs [11]	0.24 μA mM^{-1} cm^{-2}
Polypyrrole - polyanion/PEG [12]	0.[illegible]5 μA mM^{-1} cm^{-2}
MWCNT-chitosan [13]	8.3 μA mM^{-1} cm^{-2}
chitosan/PVI-Os/CNT [9]	19.7 μA mM^{-1} cm^{-2}

2 order of magnitude!!!

[9] X. Cui, *Biosensors and Bioelectronics*, vol. 22, pages 3288-3292, 2007
[11] M. Yang, *Nanotechnology*, vol. 19, page 075502, 2008
[12] W.J. Sung, *Sensors and Actuators B*, vol. 114, pages 164-169, 2006
[13] Y. Tsai, *Sensors and Actuators B*, vol. 125, pages 474-481, 2007

The peroxide detection is highly improved by using carbon nanotubes

Cottrell effect on Glucose Oxidase

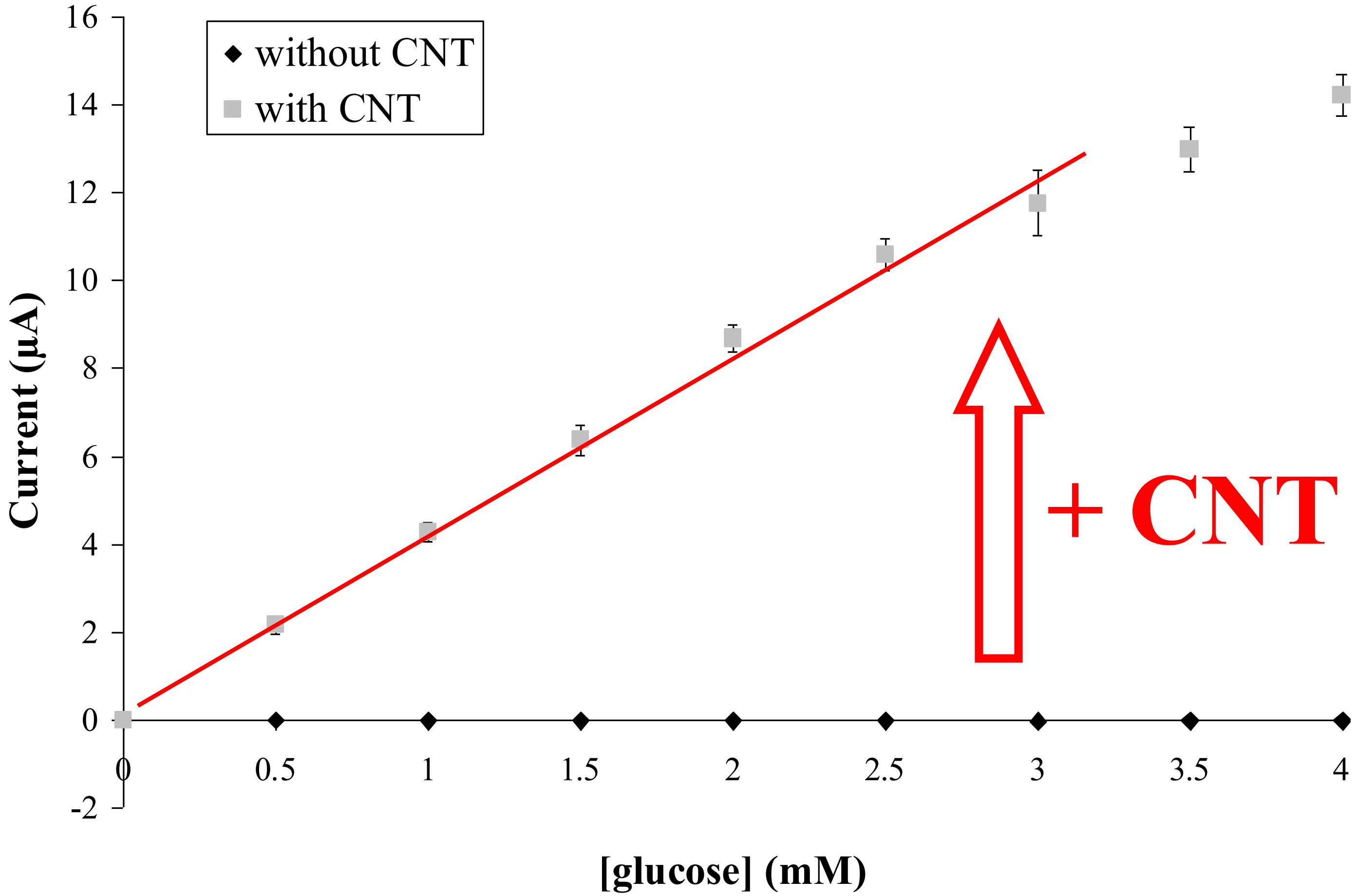

Increased Sensitivity by different techniques

		Sensitivity * [μA/(mM*cm^2)]	Limit of Detection * (LOD) [μM]
DROP CASTING	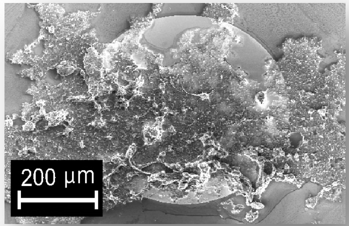	27.7 ± 0.1	73 ± 1
MICRO SPOTTING	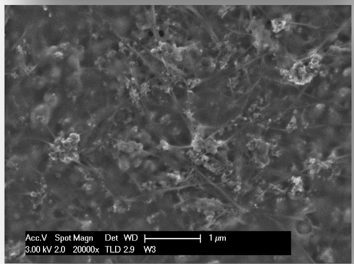	0.46 ± 2	115 ± 1
ELECTRO DEPOSITION	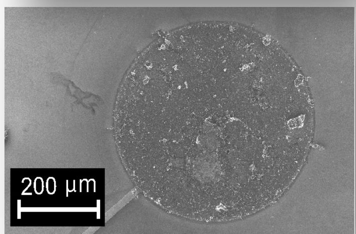	63 ± 15	8 ± 2
CVD growth	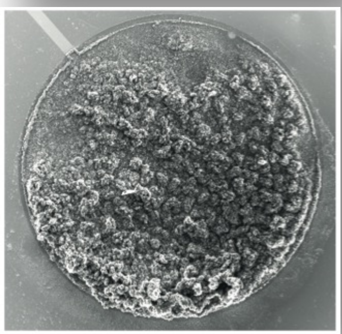	111.2 ± 0.3 (5703 ± 566	0.745 ± 0.005 3.5 ± 1.3) #

* on Glucose detection

\# on Uric Acid detection

Cottrell effect on Lactate Oxidase

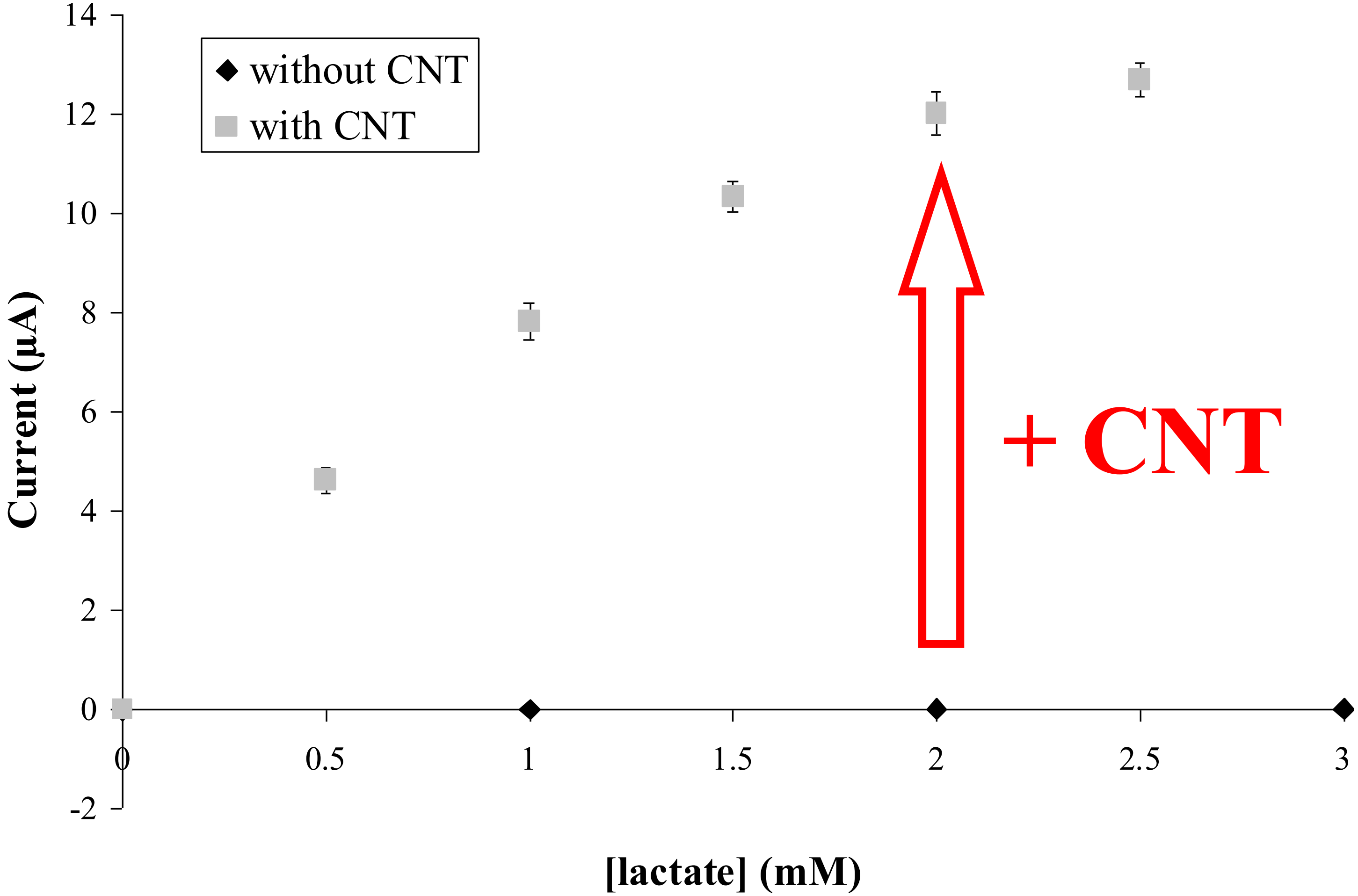

Randles-Sevçik Effect on Etoposide

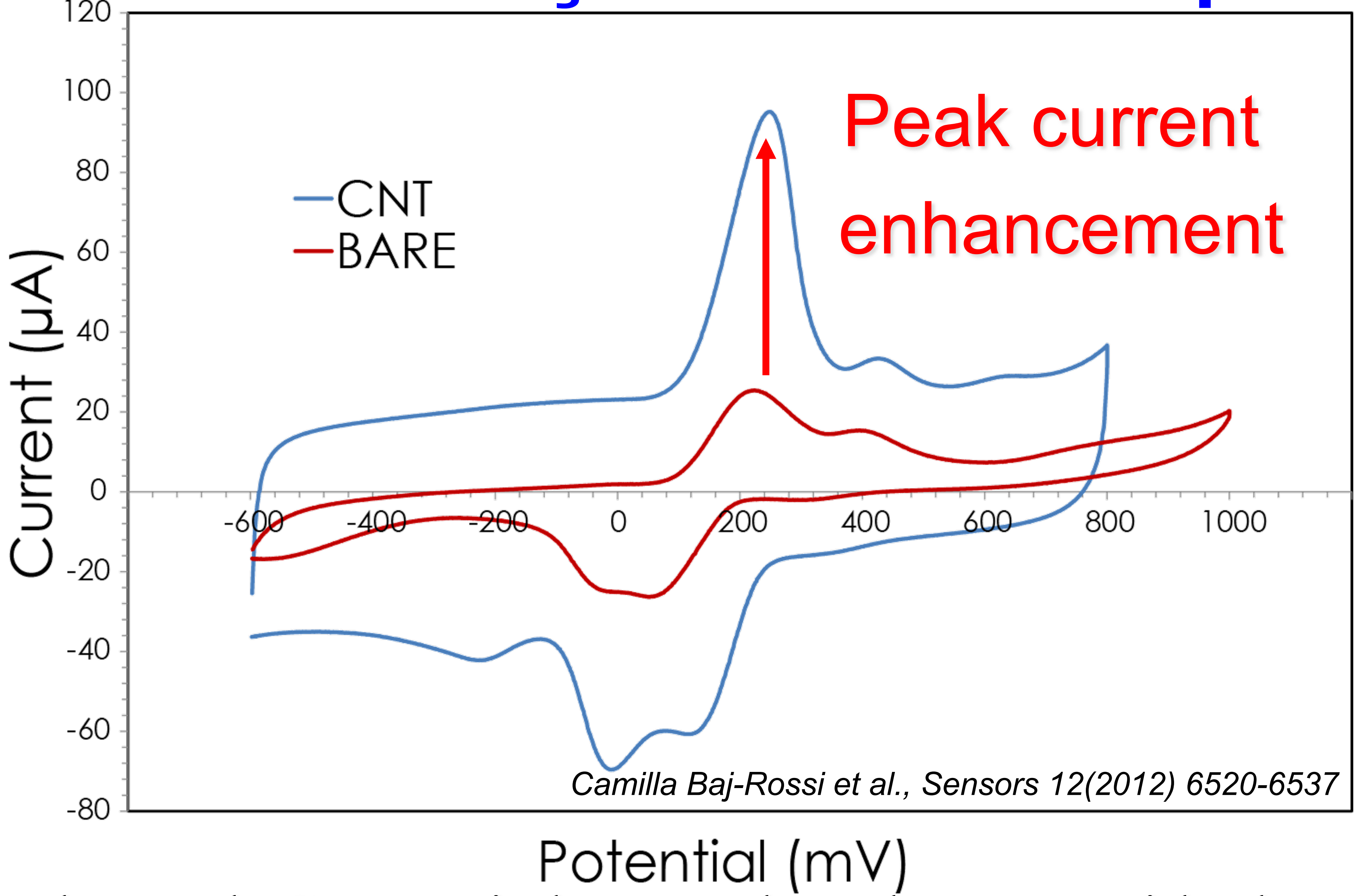

The Peak Current is larger when the Etoposide detection is mediated by Multi Walled Carbon Nanotubes

Randles-Sevçik Effect on P450

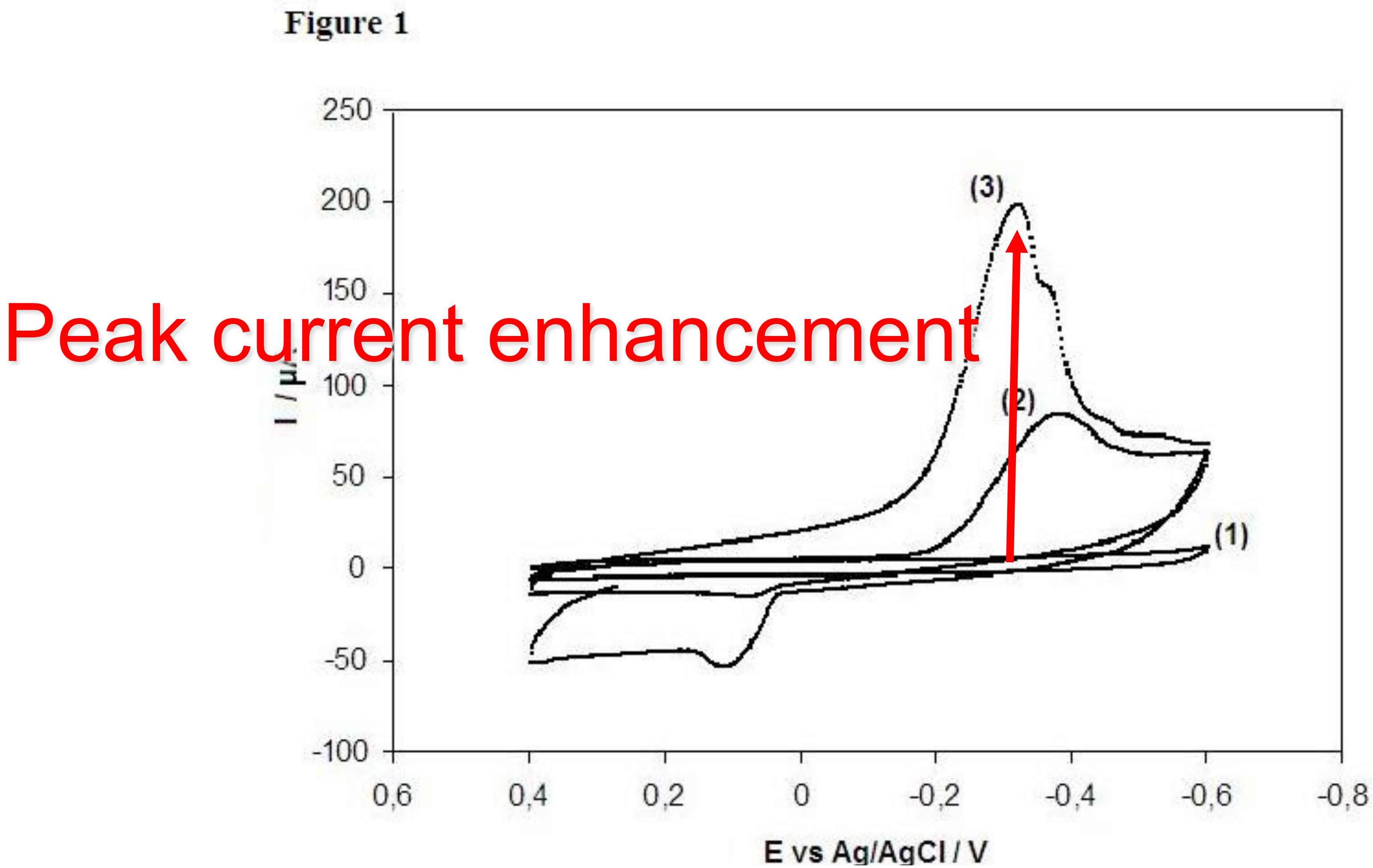

S. Carrara et al. / Biosensors and Bioelectronics 24 (2008) 148–150

The Peak Current is larger when the P450 11A1 Activity is mediated by Multi Walled Carbon Nanotubes

Randles-Sevçik on calibration

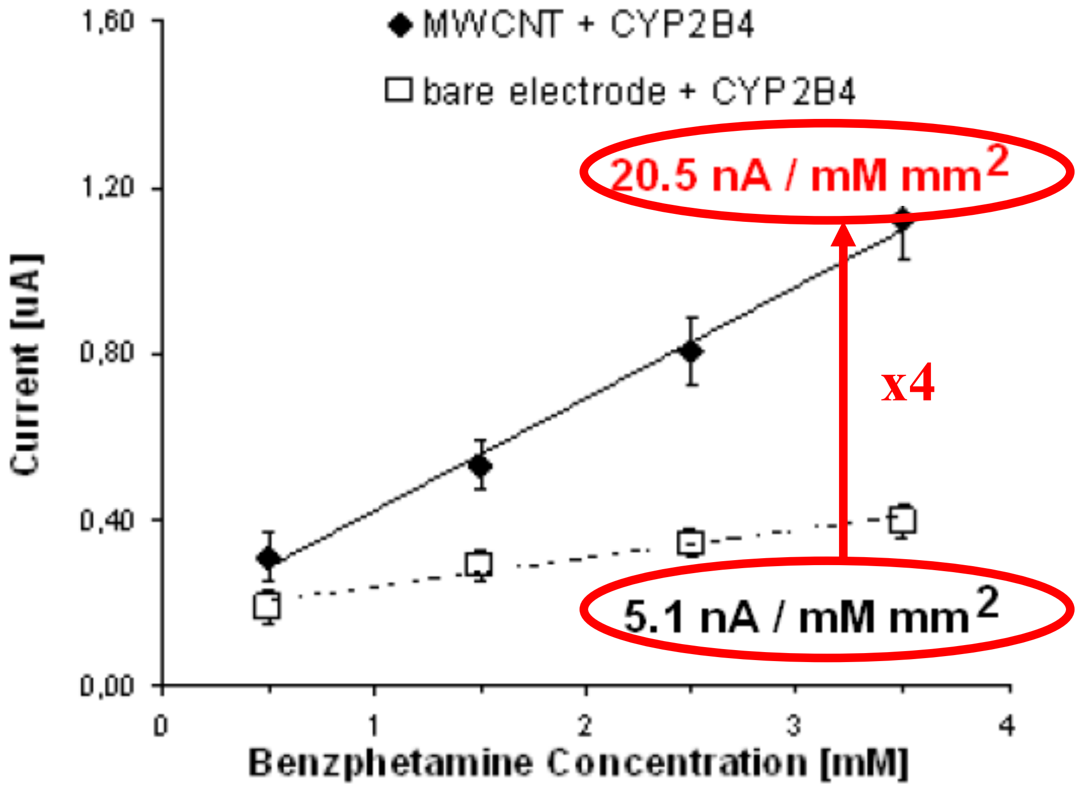

S. Carrara et al., Conference Proceedings of IEEE CME2009, Tempe (US), 9-11, April, 2009

P450 2B4 performance in detecting Benzphetamine is enhanced by a factor 4x by using MWCNT

Randles-Sevçik on calibration

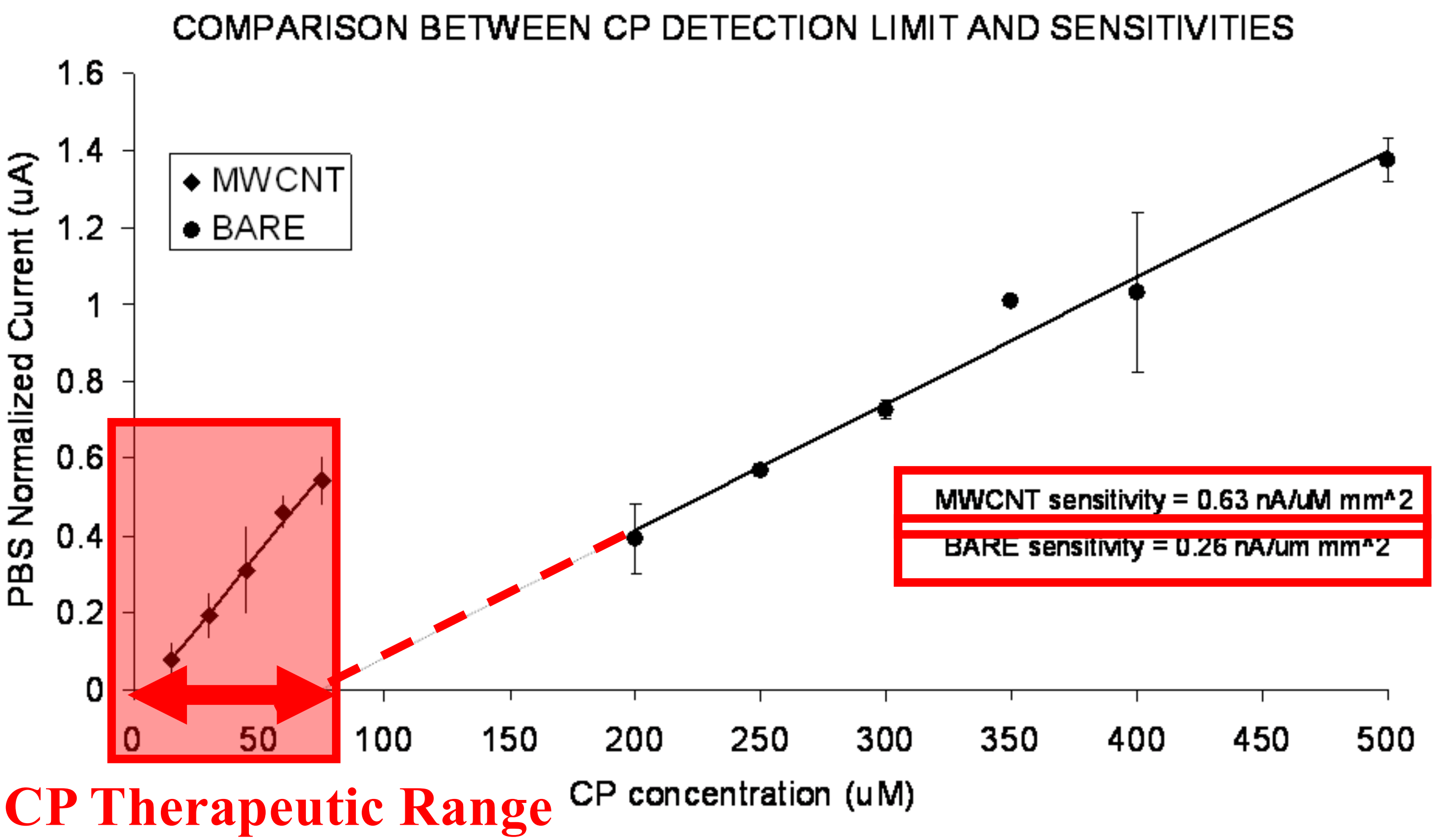

S. Carrara et al. / Biosensors and Bioelectronics 26 (2011) 3914–3919

Cyclophosphamide (CP), an anti-cancer agent, is detected by P450 3A4 in its therapeutic range